

A HYBRID METHOD FOR COMPUTING THE RCS OF WIRE SCATTERERS WITH AN ARBITRARY ORIENTATION

D.-W. Seo

Department of Electrical Engineering
KAIST
335 Gwahangno, Yuseong-gu, Daejeon 305-701, Korea

J.-H. Yoo and K. Kwon

Agency for Defense Development
Yuseong P. O. Box 35-3, Daejeon 305-600, Korea

N.-H. Myung

Department of Electrical Engineering
KAIST
335 Gwahangno, Yuseong-gu, Daejeon 305-701, Korea

Abstract—A hybrid method is proposed to compute the radar cross section (RCS) of multiple wire scatterers with an arbitrary orientation. Foldy-Lax equations in vector form are transformed into self-consistent equations for including the multiple scattering effects between scatterers. A thin-wire approximation of a method of moment (MoM) is used for calculating the scattering transition operator of a single wire scatterer. To verify the proposed method, two measurement models are fabricated and measured in a compact range chamber. The measured results agree well with the results of the proposed method.

1. INTRODUCTION

The use of chaff is the simplest radar countermeasure, in which aircrafts or warships spread a lot of small, thin metalized glass fibers. The chaff fibers are usually operating at resonance frequency and it is well

known that scatterers stay in the air for 1–2 hours with a horizontal orientation because they have a high aspect ratio (ratio of the length to the diameter of the scatterer) [1, 2]. However, chaff fibers are not aligned along one particular direction but oriented with an arbitrary orientation distribution. Consequently, the difficulty of estimating the radar cross section (RCS) of chaff fibers is that analysis region is wide, and the number of chaff fibers is large, and chaff fibers have not only a high aspect ratio but also an arbitrary orientation.

Numerous methods developed for the scattering calculation of wire scatterers are applicable to estimating the RCS of chaff fibers. Early analysis for the RCS of conducting resonant dipoles used a method of moment (MoM) [3, 4]. The MoM is one of the approaches using Maxwell's integral equation and provides a very accurate solution by virtue of considering mutual coupling between scatterers. In addition, a thin-wire approximation of the MoM provides an accurate scattering response for scatterers with a high aspect ratio [5, 6]. However, the analyzable number of wire scatterers is restricted to about several hundred due to the limitations of the computation time and computer memory. Thus, only general electromagnetic aspects of several hundred wire scatterers can be inferred.

To overcome the limited analyzable number of wire scatterers, the total RCS has been calculated by the multiplication of a single wire scatterer's average RCS and the number of wire scatterers under the assumption that the distance between wire scatterers is more than 2λ and thus mutual coupling is negligible [7, 8]. As a result, this approach does not take mutual coupling into account, and the calculation is simple and fast, but precise estimation of the RCS is not feasible. So far, the way of taking the effect of mutual coupling into account for analyzing the RCS of collective scatterers is restricted to several hundred scatterers, furthermore, excluding the effect of mutual coupling hardly provides accurate estimation. Therefore, an accurate estimation for the RCS of multiple scatterers has to consider mutual coupling and overcome the physical limitations, the calculation time and computer memory.

Conventionally, the electromagnetic scattering problem in random media with multiple particles has been investigated from the radiative transfer theory and the multiple scattering theory [9, 10]. The former is commonly used in computation of a microwave backscatter from vegetation. The radiative transfer theory is also applied to estimate the RCS of a foil cloud [16]. Similarly, the radiative transfer theory can be used for the chaff fibers' cloud. However, the main drawback of the radiative transfer theory is that it does not generally include 3rd or higher order of multiple scattering.

Multiple scattering theories have been studied extensively in the past and applied to variety of problems [9]. Early workers include Foldy [11], Lax [12], Keller [13], and Twersky [14]. Diagram method such as Dyson equation and Bethe-Salpeter equation gives a concise formal representation of the complete multiple scattering processes [15]. Among the various useful multiple scattering theories, the Foldy-Lax equations (also called the T-matrix method) are widely used method to compute the multiple scattering of multiple scatterers [9–12]. Especially, the Foldy-Lax equations have developed into recursive centered T-matrix algorithm (RCTMA) [17], null-field method [18], and so on. The T-matrix of a single scatterer relates a scattered wave to an incident wave based on spherical harmonics in the three-dimensional case. Therefore, the T-matrix provides an accurate response only for a globular scatterer with a low aspect ratio. In the case of a scatterer with a high aspect ratio, a null-field method with discrete sources can be used, but there is a problem of instability, which occurs for strongly deformed particles or large size parameters. Moreover, scatterers with an aspect ratio of 50 are barely achieved with this approach [18], while the aspect ratio of the chaff fibers ranges from 100 to 150 [1, 2].

This paper describes the development of a hybrid numerical electromagnetic modeling technique. The approach described here combines the Foldy-Lax equations with the MoM. The thin-wire approximation of the MoM is used for the scattering response of a single scatterer with a high aspect ratio and the Foldy-Lax equations are used to calculate the multiple scattering between scatterers. For verification of the proposed method, measurement models are fabricated and measured in a compact range chamber.

2. FOLDY-LAX EQUATIONS/MOM HYBRID METHOD

The classical Foldy-Lax equations have been used to calculate the multiple scattering between isotropic scatterers such as point scatterers. Let the incident exciting field on a point scatterer j be E_j^{exc} , as shown Fig. 1, then the scattered field from the point scatterer j can be represented by [10–12]

$$E_j^s = G_0 T_j E_j^{exc}, \quad (1)$$

where G_0 and T_j are the 3D free-space Green's function and the scattering transition operator of the point scatterer j , respectively.

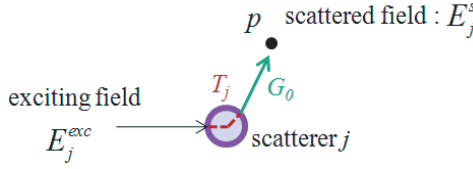


Figure 1. Characteristic parameters of Foldy-Lax equations.

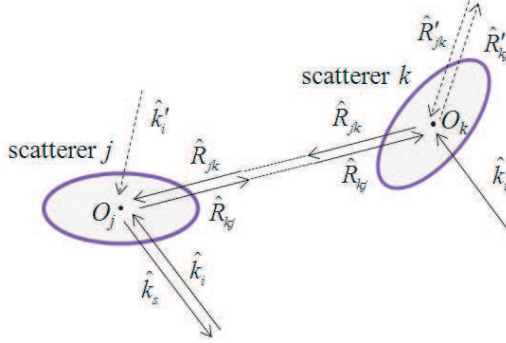


Figure 2. Two identical anisotropic scatterers with different orientations.

2.1. Self-consistent Equations of Foldy-Lax Equations for Scatterers with Different Directions

The classical Foldy-Lax equations are used for isotropic scattering problems in which the scattered field has nothing to do with the incident angle against the scatterer. The chaff fiber is not an isotropic scatterer. Thus, the Foldy-Lax equations need to be converted into a vector form to be applied to non-isotropic scatterers. That is, the incident angle and scattered angle need to be taken into account and the original Foldy-Lax equations need to be modified.

Let us consider two identical scatterers j and k whose orientations are different as shown in Fig. 2. \hat{k}_i is the unit propagation vector of the incident field and \hat{R}_{jk} is the unit vector from the scatterer k toward the scatterer j . O_j and O_k are centers of scatterers j and k , respectively. The solid line arrows denote the paths of each field and the dotted line arrows denote the coordinate conversions of the corresponding solid line arrows. In other words, if a field path enters into O_j with the direction of \hat{R}_{jk} , then the coordination-converted field path of \hat{R}_{jk} enters into O_k with the same angle, \hat{R}'_{jk} .

If a plane wave illuminates the two scatterers in the direction of \hat{k}_i , the scattered field from the scatterer j can be described as the sum of the direct scattering $\vec{G}_0 \vec{T}_j(\hat{k}_s, \hat{k}_i) \mathbf{E}^i$, the second

order scattering $\vec{G}_0\vec{T}_j(\hat{k}_s, \hat{R}_{jk})\vec{G}_0\vec{T}_k(\hat{R}_{jk}, \hat{k}_i)\mathbf{E}^i$, the third order $\vec{G}_0\vec{T}_j(\hat{k}_s, \hat{R}_{jk})\vec{G}_0\vec{T}_k(\hat{R}_{jk}, \hat{R}_{kj})\vec{G}_0\vec{T}_j(\hat{R}_{kj}, \hat{k}_i)\mathbf{E}^i$ and so on, up to an infinite number of terms. It can be represented as follows

$$\begin{aligned} \mathbf{E}_j^s(\hat{k}_s) &= \vec{G}_0\vec{T}_j(\hat{k}_s, \hat{k}_i)\mathbf{E}^i + \vec{G}_0\vec{T}_j(\hat{k}_s, \hat{R}_{jk})\vec{G}_0\vec{T}_k(\hat{R}_{jk}, \hat{k}_i)\mathbf{E}^i \\ &\quad + \vec{G}_0\vec{T}_j(\hat{k}_s, \hat{R}_{jk})\vec{G}_0\vec{T}_k(\hat{R}_{jk}, \hat{R}_{kj})\vec{G}_0\vec{T}_j(\hat{R}_{kj}, \hat{k}_i)\mathbf{E}^i \\ &\quad + \vec{G}_0\vec{T}_j(\hat{k}_s, \hat{R}_{jk})\vec{G}_0\vec{T}_k(\hat{R}_{jk}, \hat{R}_{kj})\vec{G}_0\vec{T}_j(\hat{R}_{kj}, \hat{R}_{jk}) \\ &\quad \vec{G}_0\vec{T}_k(\hat{R}_{jk}, \hat{k}_i)\mathbf{E}^i + \dots, \end{aligned} \quad (2)$$

where $\vec{T}_j(\hat{k}_s, \hat{k}_i)$ is the amount of scattered field toward \hat{k}_s when a wave is incident on the scatterer j with the direction of \hat{k}_i . \vec{G}_0 is the dyadic Green's function. In order to make (2) into self-consistent equations, the right hand side needs to be written as a multiplication of $\vec{T}_j(\hat{k}_s, \hat{k}_i)$. Thus, adjusting the order of the field path and the coordination-converted field path, we can derive the approximate expression as

$$\vec{T}_j(\hat{k}_s, \hat{R}_{jk})\vec{T}_k(\hat{R}_{jk}, \hat{k}_i) \approx \vec{T}_j(\hat{k}_s, \hat{k}_i)\vec{T}_k(\hat{R}_{jk}, \hat{R}'_{jk}), \quad (3)$$

$$\vec{T}_j(\hat{k}_s, \hat{R}_{jk})\vec{T}_j(\hat{R}_{kj}, \hat{k}_i) \approx \vec{T}_j(\hat{k}_s, \hat{k}_i)\vec{T}_j(\hat{R}_{kj}, \hat{R}_{jk}), \quad (4)$$

$$\vec{T}_k(\hat{R}_{jk}, \hat{R}_{kj})\vec{T}_j(\hat{R}_{kj}, \hat{R}_{jk}) \approx \vec{T}_k(\hat{R}_{jk}, \hat{R}'_{jk})\vec{T}_k(\hat{R}_{jk}, \hat{R}'_{jk}). \quad (5)$$

Using the above approximations, (2) can be simplified as

$$\begin{aligned} \mathbf{E}_j^s(\hat{k}_s) &\approx \vec{G}_0\vec{T}_j(\hat{k}_s, \hat{k}_i)\left\{\mathbf{E}^i + \vec{G}_0\vec{T}_k(\hat{R}_{jk}, \hat{R}'_{jk})\mathbf{E}^i \right. \\ &\quad + \vec{G}_0\vec{T}_k(\hat{R}_{jk}, \hat{R}'_{jk})\vec{G}_0\vec{T}_k(\hat{R}_{jk}, \hat{R}'_{jk})\mathbf{E}^i \\ &\quad \left. + \vec{G}_0\vec{T}_k(\hat{R}_{jk}, \hat{R}'_{jk})\vec{G}_0\vec{T}_k(\hat{R}_{jk}, \hat{R}'_{jk})\vec{G}_0\vec{T}_k(\hat{R}_{jk}, \hat{R}'_{jk})\mathbf{E}^i + \dots\right\} \\ &\approx \vec{G}_0\vec{T}_j(\hat{k}_s, \hat{k}_i)\mathbf{E}_j^{exc}. \end{aligned} \quad (6)$$

Then, the exciting field of the scatterer j with arbitrary orientation can be represented as follows

$$\mathbf{E}_j^{exc} \approx \mathbf{E}^i + \vec{G}_0\vec{T}_k(\hat{R}_{jk}, \hat{R}'_{jk})\mathbf{E}_k^{exc}. \quad (7)$$

If the self-consistent equations for two scatterers are extended to N scatterers, a problem generalization can be made as

$$\mathbf{E}_j^{exc} \approx \mathbf{E}^i(\hat{k}_i) + \sum_{\substack{k=1 \\ k \neq j}}^N \vec{G}_0 \vec{T}_k(\hat{R}_{jk}, \hat{R}'_{jk}) \mathbf{E}_k^{exc}. \quad (8)$$

In (8), it can be intuitively seen that the exciting field of the scatterer j is the summation of the incident field and all scattered fields heading to the scatterer j from neighboring scatterers. If the second term of the right hand side is tied over the left hand side, the Equation (8) can now be written as

$$\left[I - \sum_{\substack{k=1 \\ k \neq j}}^N \vec{G}_0 \vec{T}_k(\hat{R}_{jk}, \hat{R}'_{jk}) \right] \mathbf{E}_k^{exc} \approx \mathbf{E}^i(\hat{k}_i). \quad (9)$$

If we further let

$$Z_{jk} = \begin{cases} 1 & \text{if } j = k \\ -\vec{G}_0 \vec{T}(\hat{R}_{jk}, \hat{R}'_{jk}) & \text{if } j \neq k \end{cases}, \quad (10)$$

then we have the following matrix equation:

$$\sum_{k=1}^N Z_{jk} \mathbf{E}_k^{exc} \approx \mathbf{E}^i(\hat{k}_i). \quad (11)$$

In matrix notation

$$\overline{\overline{Z}} \cdot \overline{\overline{E}}^{exc} = \overline{\overline{E}}^i, \quad (12)$$

where $\overline{\overline{Z}}$ is the interaction matrix that contains the interaction between scatterers and is independent of both the incident and scattered angle, $\overline{\overline{E}}^{exc}$ is the unknown vector of the exciting fields of the scatterers, and $\overline{\overline{E}}^i$ is the known vector of the incident fields.

The interaction matrix has a $N \times N$ dimension and is symmetric. If the upper triangular entries of $\overline{\overline{Z}}$ are known, the lower parts can be obtained without the calculation of the scattering transition operators. Therefore, the calculation time can be reduced. If the distance between neighboring wire scatterers is greater than 2λ , then the effect of mutual coupling can be negligible [19]. To reduce the calculation time, assume that there is no mutual coupling when the center distance between the chaff fibers is greater than 2λ . Therefore, the interaction matrix is

approximately obtained as

$$Z_{jk} = \begin{cases} 1 & \text{if } j = k \\ 0 & \text{if } j > k \text{ and } R_{jk} \geq 2\lambda \\ -\vec{G}_0 \vec{T} \left(\hat{R}_{jk}, \hat{R}'_{jk} \right) & \text{if } j > k \text{ and } R_{jk} < 2\lambda \\ Z_{kj} & \text{if } j < k \end{cases} \quad (13)$$

The case of the exciting fields of N -scatterers can be directly obtained through the matrix calculation, then the total scattered field can be found by using

$$\mathbf{E}^s \left(\hat{k}_s \right) = \sum_{j=1}^N \mathbf{E}_j^s \left(\hat{k}_s \right) = \sum_{j=1}^N \vec{G}_0 \vec{T}_j \left(\hat{k}_s, \hat{k}_i \right) \mathbf{E}_j^{exc}, \quad (14)$$

where \hat{k}_s is the direction toward the observation point.

2.2. Scattering Transition Operator, $\vec{T} \left(\hat{k}_s, \hat{k}_i \right)$

For a single isotropic scatterer, the scattering transition operator as a response of the scatterer by the exciting field generally has a fixed constant value. However, the wire scatterer is anisotropic. Thus, the scattering transition operator must be expressed in terms of the exciting angle, scattered angle, and polarization as follows

$$\vec{T} \left(\hat{k}_s, \hat{k}_i \right) = \begin{bmatrix} T_{\theta\theta} \left(\theta^s, \phi^s; \theta^{exc}, \phi^{exc} \right) & T_{\theta\phi} \left(\theta^s, \phi^s; \theta^{exc}, \phi^{exc} \right) \\ T_{\phi\theta} \left(\theta^s, \phi^s; \theta^{exc}, \phi^{exc} \right) & T_{\phi\phi} \left(\theta^s, \phi^s; \theta^{exc}, \phi^{exc} \right) \end{bmatrix}, \quad (15)$$

where θ^{exc} , ϕ^{exc} , θ^s , and ϕ^s are the exciting (or incident) zenith angle, azimuth angle, scattered zenith angle, and azimuth angle with respect to a single scatterer, respectively. Each component in the scattering transition operator implies a scattered field whose polarization is in the direction of interest when a unit incident field (magnitude of 1) illuminates the scatterer in a fixed direction \hat{k}_i .

The transition operator can be derived by various methods [5, 6, 20, 21] that consider the exciting angle, scattered angle, and polarization. Partial differential equation (PDE) techniques such as a finite element method (FEM) have to employ an absorbing boundary in order to model an unbounded radiating structure. On the other hand, surface integral techniques such as the MoM and a boundary element method are very efficient for solving open radiation problems involving thin wires. Among various surface integral techniques, the MoM requires the determination of an impedance matrix indicating the scattering information of the scatterer. Using the thin-wire approximation, we can calculate the impedance matrix of a single scatterer

with a high aspect ratio easily and accurately. Once the matrix is obtained, we can repeatedly work on any identical scatterer regardless of the exciting angle, scattered angle, and polarization. Therefore, the MoM is used to calculate the scattering transition operator expressed in the matrix form as (15). The elements of the scattering transition operator are obtained by

$$T_{pq}(\theta^s, \phi^s; \theta^{exc}, \phi^{exc}) = \frac{-jk_0\eta}{4\pi r} e^{-jk_0r} \mathbf{R}_p^T \mathbf{Z}^{-1} \mathbf{V}_q, \quad (16)$$

where η is the intrinsic impedance. The subscripts p and q can be either θ or ϕ ($p, q = \theta, \phi$). The first subscript specifies the polarization of the scattered wave and the second the polarization of the exciting wave. \mathbf{Z} is the impedance matrix of a single wire and T is the transpose operator. \mathbf{R} and \mathbf{V} are the measurement vector and excitation vector, respectively. Information about the incident angle and polarizations is included in the measurement vector \mathbf{R} , and information about the scattered angle and polarizations is included in the exciting vector \mathbf{V} . The MoM is implemented using Galerkin's method.

2.3. Flow Chart

Figure 3 describes the general calculation process for the proposed hybrid method. First, the radar information, frequency, the incident, and scattering angle, must be acquired, and the information about the scatterers, the length, location, and direction, needs to be inputted. Here, the location of the scatterer is defined as the absolute coordinate of the scatterer's center point, while the orientation is represented by the zenith angle and azimuth angle. The orientation of the scatterer in analysis might be different but the impedance matrix of a single scatterer is calculated only once since the shape of the chaff fibers is identical. The single chaff fiber is divided into 4 segments and the impedance matrix is constructed.

Then, the Foldy-Lax equation implying the mutual coupling effect is configured. At this time, the scattering transition operator regarding the incident angle, scattered angle, and polarization is calculated using the previously found impedance matrix. The composed Foldy-Lax equation can be converted into a matrix expression and then the exciting field can be found. The matrix equation of (12) is solved using the LU decomposition. However, a scattering matrix method, such as T-matrix, can be accelerated by the iterative method [17, 22] or the fast multipole method (FMM) [23]. Therefore, the proposed hybrid method can also be solved using the acceleration techniques.

Finally, the total scattered field can be found with the calculated exciting field.

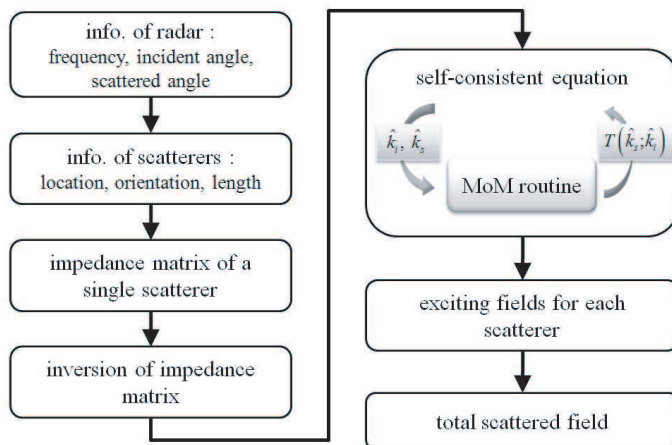


Figure 3. Flow chart of the proposed method.

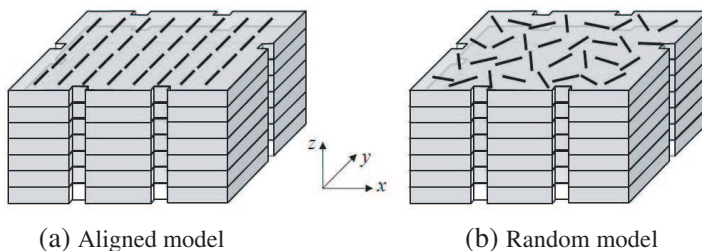


Figure 4. Measurement models.

3. MEASUREMENT AND NUMERICAL RESULTS

To validate the proposed method, the calculation results are compared with the measured backscattering RCS. In addition, we prepare the additional data which is calculated from the MoM to verify accuracy that is free of measurement error. Two models are fabricated for the measurement: (1) aligned model (2) random model as shown in Fig. 4. The aligned model contains identical wire scatterers with the same orientation. For the random model, the elevation angles of wire scatterers are the same as 90° but the azimuth angles of wire scatterers are set by a uniform random generator with a range of $0-360^\circ$.

The length and aspect ratio of wire scatterers are 5 cm and 153.8, respectively. The resonance frequency of these wire scatterers is 3 GHz and a total of 224 wire scatterers in the form of an $8 \times 4 \times 7$ array are immersed in $42 \times 30 \times 35 \text{ cm}^3$ Styrofoam without using adhesive

tape. The gaps between adjacent wires are 5 cm, 7–8 cm, and 0.49 cm along the x , y -, and z -axis, respectively. In order to align and fix the layers, Styrofoam sticks are inserted into grooves in the sides. The relative permittivity of the Styrofoam is about $1.03-j0.0001$ at 3 GHz and is not considered in the analysis. The material of wire is iron with a conductivity of about 10^7 S/m and is considered a perfectly conducting wire in the analysis. The RCSs of two measurement models are estimated by the proposed method and the MoM employing MATLAB 7.8 with a 2.83 GHz Quad CPU and a 8 Gbyte RAM PC.

Since all the wires are oriented horizontally, the backscattering RCS for the horizontal polarizations of the transmitter and receiver is measured when an incident field illuminates with $\theta^i = 90^\circ$ and $\phi^i = 0-360^\circ$. Figs. 5 and 6 show the measured and calculated $\phi - \phi$ polarization backscattering RCS as a function of the incident angle at resonance frequency for both models. In Fig. 5, typical disparities between the calculated and measured patterns are about 1.5 dB, except in the vicinity of nulls. The inaccuracy in the vicinity of nulls at 90° and 270° is caused by a very low measurement level. The results of the MoM also have some difference from the measured results in the vicinity of nulls. Since all the wires are oriented parallel to the y -axis, there is no wire component in x -direction. For the incident wave with $\phi^i = 90^\circ$ or 270° , ϕ -polarization is the same as x -polarization according to the coordinate transformation. Thus, $\sigma_{\phi\phi}$ has a null value at $\phi^i = 90^\circ$ and 270° .

Figure 6 shows the results of the proposed method and measurement for the random model. In terms of the peaks and nulls of the RCS, the results of the proposed method are in good agreement with the measurements as well as with the results of the MoM.

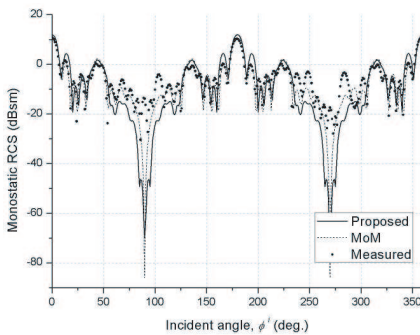


Figure 5. Backscattering RCS for the aligned model with $\theta^i = 90^\circ$ at $f = 3$ GHz.

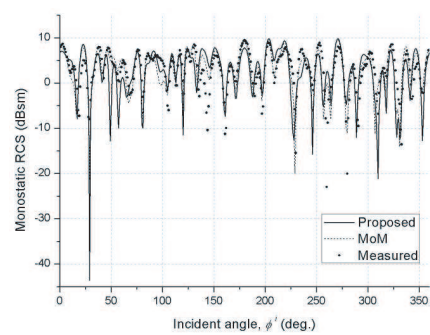


Figure 6. Backscattering RCS for the random model with $\theta^i = 90^\circ$ at $f = 3$ GHz.

Table 1. nMSE for the proposed method and the MoM.

<i>Model</i>	<i>Measured results as reference</i>		<i>MoM results as reference</i>	
	<i>Method</i>	nMSE	<i>Method</i>	nMSE
Aligned model	MoM	0.1314	Proposed	0.0202
	Proposed	0.1863		
Random model	MoM	0.1356	Proposed	0.0973
	Proposed	0.2762		

In order to measure the differences between calculated RCSs and measured RCSs, the normalized mean square error (nMSE) is often used. It is defined as

$$nMSE = \frac{\sum_{n=1}^N |RCS_n^p - RCS_n^r|^2}{\sum_{n=1}^N |RCS_n^r|^2} \quad (17)$$

where RCS_n^p is the linear scaled RCS estimated by the proposed method and the MoM, and RCS_n^r is the measured linear scaled RCS as reference value at the n th incident angle. Table 1 presents the nMSE for the proposed method and the MoM. In the case of using the measured data as reference values, the accuracy by the MoM is little more than the proposed method. But if reference values are results of the MoM that is free of measurement error, it can be seen that the proposed method have very small nMSE and considerably give accurate value.

Table 2 summaries the CPU times and required matrix size for each fabricated model and each applied calculation method. The proposed method is about 160 times faster than the MoM for estimating the RCS of the aligned model. Clearly, the proposed method shows great improvement in time against the MoM approach. For the random model, on the other hand, the proposed method was about 30 times faster than the MoM. The main reason for the different calculation time is that all the wires have identical $\vec{T}_j(\hat{k}_s, \hat{k}_i)$ in (14) for the aligned model. In Table 2, the size means the memory size, dimension of the impedance matrix for the MoM and the matrix arising from (8) for the proposed method. Because a single wire is divided into 4 segments, the impedance matrix \mathbf{Z} in (16) is a 4 by 4 matrix with 256 bytes for a single wire. The size of the interaction matrix from (13) is 784 Kbytes, while the size of the impedance matrix by the MoM is 12,544 Kbytes.

Table 2. CPU time and memory for computing the RCS of measurement model.

<i>Model</i>	<i>Method</i>	<i>CPU time</i> (<i>sec.</i>)	<i>Size (dim.)</i>	<i>Size (Kbyte)</i>
Aligned model	MoM	3,433.1	896×896	12,544
	Proposed	20.9	224×224	784
Random model	MoM	3,475.4	896×896	12,544
	Proposed	102.9	224×224	784

4. CONCLUSION

To compute the multiple scattering between scatterers with a high aspect ratio, under the assumption that identical scatterers have arbitrary directions, the self-consistent equations (in vector form) of the Foldy-Lax equation was formulated by re-ordering the field path and the coordination-converted field path. The scattering transition operator was derived by the thin-wire approximation of the MoM. That is, the hybrid method using the Foldy-Lax equations and the MoM was proposed. For verification, measurement models were fabricated and measured. Compared to the results of the measurement, the results of the proposed method showed good accuracy. The proposed hybrid method is useful for estimating the RCS of a group of more than several thousand wire scatterers. Besides, the proposed method is applicable to estimated electromagnetic scattering of periodic conducting wires such as FSS (frequency selective surface), EBG (electromagnetic band-gap), and negative permittivity meta-materials. Especially, it expected to estimate the characteristics of the fiber-filled composite. In addition to, the proposed method can be applicable to RCS calculation for not only wire scatterers but also multiple scatterers with any identical shape.

ACKNOWLEDGMENT

This research was supported by the Agency for Defense Development, Korea, through the Radiowave Detection Research Center at KAIST.

REFERENCES

1. Butters, B. C. F., "Electronic countermeasures/chaff," *IEEE Proceedings*, Vol. 129, No. 3, Part F, 197–201, June 1982.

2. Arnott, W. P., A. Huggins, J. Gilles, D. Kingsmill, and J. Walker, "Determination of radar chaff diameter distribution function, fall speed, and concentration in the atmosphere by use of the NEXRAD radar," *Desert Research Institute*, Reno, USA, 2004.
3. Wickliff, R. and R. Garbacz, "The average backscattering cross section of clouds of randomized resonant dipoles," *IEEE Trans. Antennas and Propagat.*, Vol. 22, No. 3, 503–505, May 1974.
4. Cuevas, A., "The method of relative phase applied to wire-type scattering structures," *IEEE AP-S Int. Symp.*, Vol. 3, 1516–1519, 1991.
5. King, R. W. P., *Table of Antenna Characteristics*, Plenum Press, 1971.
6. Wang, J. J. H., *Generalized Moment Methods in Electromagnetics*, Wiley, New York, 1991.
7. Macedo, A. D. F., "Analysis of chaff cloud RCS applying fuzzy calculus," *1997 SBMO/IEEE MTT-S*, Vol. 2, No. 11–14, 724–728, August 1997.
8. Pouliguen, P., O. Bechu, and J. L. Pinchot, "Simulation of chaff cloud radar cross section," *IEEE AP-S Int. Symp.*, Vol. 3A, No. 3–8, 80–83, July 2005.
9. Ishimaru, A., *Wave Propagation and Scattering in Random Media*, Wiley-IEEE Press, 1994.
10. Tsang, L., J. A. Kong, K.-H. Ding, and C. O. Ao, *Scattering of Electromagnetic Waves: Numerical Simulation*, Wiley-Interscience, 2004.
11. Foldy, L. O., "The multiple scattering of waves," *Phys. Rev.*, Vol. 67, 107–109, 1945.
12. Lax, M., "Multiple scattering of waves," *Rev. Mod. Phys.*, Vol. 23, 287–310, 1951.
13. Keller, J. B., "Stochastic equations and wave propagation in random media," *Proc. Symp. in Appl. Math.*, Vol. 16, 145–170, 1964.
14. Twersky, V., "On propagation in random media of discrete scatterers," *Proc. Amer. Math. Soc. Symp. on Stochastic Process in Mathematical Physics and Engineering*, Vol. 16, 84–116, 1964.
15. Frisch, U., "Wave propagation in random media," *Probability Methods in Applied Mathematics*, A. T. Bharucha-Reid (ed.), Vol. 1, 76–198, Academic Press, New York, 1968.
16. Zhang, M., Z. S. Wu, and K. X. Liu, "Monte carlo simulations of the EM bistatic scattering from a novel foil cloud," *5th International Symposium on Antennas, Propagation and EM*

- Theory*, 45–49, Beijing, China, Aug. 15–18, 2000.
17. Auger, J.-C. and B. Stout, “A recursive centered T-matrix algorithm to solve the multiple scattering operation: Numerical validation,” *Journal of Quantitative Spectroscopy & Radiative Transfer*, 533–547, 2003.
 18. Pulbere, S. and T. Wriedt, “Light scattering by cylindrical fibers with high aspect ratio using the null-field method with discrete sources,” *Part. Part. Syst. Charact.*, Vol. 21, 213–218, 2004.
 19. Wickliff, R. and R. Garbacz, “The average backscattering cross section of clouds of randomized resonant dipoles,” *IEEE Transactions on Antennas and Propagation*, Vol. 22, No. 3, May 1974.
 20. Illahi, A., M. Afzaal, and Q. A. Naqvi, “Scattering of dipole field by a perfect electromagnetic conductor cylinder,” *Progress In Electromagnetics Research Letters*, Vol. 4, 43–53, 2008.
 21. Hatamzadeh-Varmazyar, S. and M. Naser-Moghadasi, “New numerical method for determining the scattered electromagnetic fields from thin wires,” *Progress In Electromagnetics Research B*, Vol. 3, 207–218, 2008.
 22. Gurel, L. and W. C. Chew, “Scattering solution of three-dimensional array of patches using the recursive T-matrix algorithms,” *IEEE Microwave and Guided Wave Letters*, Vol. 2, No. 5, 182–184, 1992.
 23. Zhang, Y. J. and E. P. Li, “Fast solution of foldy-lax equation for two-dimensional radiation and scattering problems,” *17th Int. Symp. on EMC*, 208–211, Zurich, 2006.